Nondestructive Evaluation of Ceramic Candle Filters Using Vibration Response [1]

Roger H.L. Chen, Associate Professor (hchen@wvu.edu; 304-293-3031 x.631)
Alejandro C. Kiriakidis, Research Assistant (304-293-3031 x.434)
Steve W. Peng, Research Assistant (304-293-3031 x.434)
Department of Civil and Environmental Engineering
West Virginia University
Morgantown, WV 26506 - 6103

Introduction

A structure's dynamic behavior is defined by a discrete spectrum of an infinite number of natural frequencies and corresponding mode shapes, which are determined by geometry, distribution of mass, stiffness and boundary conditions. Within these parameters, changes in the stiffness are directly related to changes in the safety conditions of the structure (Chen, et al.1995). This paper presents an on-going research study of nondestructive evaluation of ceramic candle filters using a dynamic characterization method. Ceramic candle filters play a key role in advanced coal-based gas turbine. They protect the heat exchanger and gas turbine components from getting clogged, and they also prevent erosion due to particle impaction. Previous studies of used ceramic filters indicate that the damage of the filters resulted from strength degradation due to thermal transient events, excessive ash accumulation, bridging, and pulse cleaning (Alvin et al., 1994). The candle filter is a hollow cylindrical structure made of porous materials, which has high acoustic attenuation, and has limited the conventional ultrasonic detection capability.

Twelve new Coors alumina mullite filters were tested. These filters have the same nominal weight and dimensions. The nominal weight is 8.4 lb (3.82 kg). and the nominal dimensions are 59.8 in (1.52 m) length and 2.36 in (60 mm) outer diameter and 1.57 in (40 mm) inner diameter. Several of these filters present initial curvatures along the longitudinal axis. The evaluation of experimental results is based on two vibration parameters: frequency shifts and mode shapes. The results will be used to develop a nondestructive inspection tool of the ceramic candle filters.

Four- point bending tests were conducted on seven filters, which include five used Schumacher filters, one new Schumacher and one new Refractron filter. The load-deflection (P- Δ) curve was measured up to 45lb (200N) of each filter. The P- Δ curve was linear between 25.7lb (114N) to 35.7lb (159N), and the stiffness of each filter was calculated using the (P- Δ) curve. The results show that the stiffness difference of these filters agrees well with the results from their vibration tests. Vibration test of a damage

[1] Research sponsored by the Federal Energy Technology Center, Department of Energy, under contract DE-FG21-97MC34160 and DE-AP21-96MC29319 with the Department of Civil and Environmental Engineering, West Virginia University, Morgantown WV 26506-6103; fax: 304-293-7109[1]

Schumacher filter was also conducted. The measured frequencies and mode shapes are found sensitive to reflect the artificially induced defect.

Objective

This study aims at the development of an effective nondestructive evaluation technique to predict the remaining useful life of a ceramic candle filter during a power plant's annual maintenance shutdown. The objective of the present on-going study is to establish the vibration signatures of ceramic candle filters at varying degradation levels due to different operating hours, and to study the various factors involving the establishment of the signatures.

Vibration Test of Coors Filters

Experiments and Analysis

An experimental setup with a rectangular shaped steel framework was used as shown in figure 1. Each one of the Coors alumina mullite filters was suspended freely by its open end (head) by using elastic tubes tied at the top of the frame, to simulate a free-free boundary condition (Figure 1). The filter was subjected to an excitation by using an impact hammer, and the response was picked up by an accelerometer, which was located at 0.55 length from the head of the filter. Impact was given at L/10, L/5, 3L/10, 2L/5, L/2, 3L/5, 7L/10, 4L/5, 9L/10, and L, where L is the length of the filter. Both input and output waveforms were stored in a digital oscilloscope and then processed by using a signal processing software. Fast Fourier Transform (FFT) was performed on the signals to get the Frequency Response Function (FRF). The FRF is obtained by taking the imaginary part of the complex function. The FRF shows a plot with various peaks that correspond to the natural frequency of vibration in different modes. The first eight flexural vibration modes, covering a frequency range up to 0-3100 Hz, were studied. A typical FRF plot is shown in Figure 2. From the FRF plots the frequency and amplitude values were noted and the mode shapes were constructed. The frequencies obtained were averaged to minimize experimental errors arising from improper impacts. Figure 3 shows the first four mode shapes measured from a typical Coors filter.

Analysis using a dynamic Finite Element Method (FEM) was conducted to compare with the experimental results. An FEM model was built for the Coors filters by using the nominal weight and dimensions. Linear elastic modal analysis was performed. Eight nodes, three-dimensional isotropic solid elements, were used. Some parametric studies were conducted on the influence of various material properties, i.e. Poisson's ratio and Young's Modulus. To study the effect of the initial curvatures that several filters present, FEM modal analysis was conducted by using 3-D beam element.

Results

Table 1 shows the first eight flexural vibration modes for each of the twelve Coors ceramic candle filters tested and the averaged frequency of each vibration mode. The Coefficient of Variation (COV) of frequency has a range between 1.41 and 1.55 for the eight different modes. Figure 4 shows the COV for the eight different modes, and the COV of each mode maintains as a constant of about 1.5. A three-dimensional Coors filter model consisting of 2208 brick elements with 4178 nodes was conducted. The FEM result using a weight density of 0.0623 lb/in^3 (1.724 g/cc) shows that the Young's modulus (E) value obtained for the Coors filters is $E = 4.26 \times 10^6$ psi (2.99×10^9 Pa).

Table 1 Experimental Vibration Frequencies Results for the Coors Filters.

Mode #	KC013 FREQ. (Hz)	KC014 FREQ. (Hz)	KC015 FREQ. (Hz)	KC016 FREQ. (Hz)	KC025 FREQ. (Hz)	KC026 FREQ. (Hz)	KC028 FREQ. (Hz)	KC029 FREQ. (Hz)	KC030 FREQ. (Hz)	KC031 FREQ. (Hz)	KC032 FREQ. (Hz)	LC023 FREQ. (Hz)	AVE.
1	111.4	110.0	114.4	112.9	111.4	110.0	112.9	112.9	114.4	111.2	109.9	113.7	112.1
2	303.5	300.3	311.6	306.7	302.0	300.6	306.4	307.2	311.3	303.6	300.6	311.4	305.4
3	584.1	582.0	602.7	590.5	584.3	573.9	591.9	593.6	602.7	585.9	581.4	599.7	589.4
4	947.6	941.5	973.4	958.3	943.0	930.8	958.3	959.3	970.5	944.7	936.9	967.4	952.6
5	1374.8	1364.1	1413.0	1391.6	1371.8	1352.1	1391.6	1390.1	1406.9	1371.8	1364.1	1408.4	1383.3
6	1855.5	1840.7	1907.3	1876.8	1847.8	1828.0	1875.4	1878.7	1901.2	1852.4	1838.7	1895.1	1866.5
7	2392.9	2348.5	2461.1	2420.0	2383.4	2365.3	2429.8	2432.6	2449.0	2386.6	2369.5	2446.6	2407.1
8	2950.4	2915.8	3035.0	2986.8	2945.3	2916.1	2966.3	2997.3	3022.5	2954.1	2925.1	3027.3	2970.2

Figure 5 shows the comparison between the experimental averaged frequencies and Finite Element (FE) calculated frequency for all the eight modes. For these filters a maximum percentage difference between the experimental and FEM results using the three different Poisson's ratios $\nu = 0.30$, $\nu = 0.20$ and $\nu = 0.15$ are 0.58%, 0.22%, and 0.49% respectively. In this figure, the X-axis represents the vibration mode number and the Y-axis represents the frequency of vibration in Hz. The FEM calculation agrees well with the experimental results. The influence on the vibration frequency of the filters from Poisson's ratio is minimal. The results also show that the 3-D FEM model used can accurately reproduce the vibration response of the Coors candle filters.

FEM calculations were also conducted to determine the influence of the initial curvatures on the ceramic candle filters. The curvatures simulated in the FEM beam elements model are higher than the real curvatures presented on the filters. The maximum calculated percentage difference in frequency between the straight filter model and the curved filter model is less than 0.4%. These low percentage differences indicate that the influence of the initial curvature on the vibration frequencies is minimal.

Bending and Vibration Tests of Used Candle Filters

Experiments and Analysis

The testing setup used for the bending experiments includes a loading frame, a 6.5 ft. (1.98 m) long steel I-beam, a 1.5 ft. (0.48 m) long aluminum I-beam, four U-shape blocks, a load cell, and a LVDT. The LVDT has a range of ± 0.05 in. of deflection. A simple bending test setup sketch is shown in figure 6.

Each Schumacher filter had a length of 59.6 in (1.51 m), an outer diameter of 2.36 in (60 mm) and an inner diameter of 1.18 in (30 mm) with a closed end wall thickness of 1.4 in (36 mm). A new Refractron ceramic candle filter with 2.36 in (60 mm) outer diameter and 1.57 in (40mm) inner diameter with a closed end wall thickness of 0.98 in (25 mm) was also tested.

At each bending test, the filter specimen was pre-loaded to 20.7 lb (92 N), which included the weight of the aluminum I-beam and two U-shape blocks of 10.7 lb (48 N) and an applied load of 10 lb (44 N). The deflection was measured from 20.7 lb (92 N) to 45.7 lb (203.3 N) at 5 lb (22.2 N) increment. At each loading, the LVDT was used to measure the deflection. Each filter was tested repeatedly four times.

A Schumacher filter, specimen number A-4, was broken into two pieces, one piece was 31.5 in (80 cm) and the other was 28 in (71 cm). These two pieces of A-4 filter were glued together using epoxy. The weight of the A-4 Schumacher was 6.605 kg before broken and 6.61 kg after repair.

The A-4 specimen was tested under vibration. The sensor was placed at the position of 0.55L of the filter, and the impact positions were L/8, L/4, L/3, 5L/12, L/2, 0.55L, 2L/3, 3L/4 and 7L/8. The damaged location was between L/2 and 0.55L. A sampling rate of 20 microsecond was used, and the FRF has a resolution of 1.5 Hz.

Results

Figures 7 shows the typical load-deflection curve of Schumacher filters specimen A-29 and B-27. In these figures, the X-axis represents loads in pounds, and the Y-axis represents deflections in inches. It can be seen from these figures that the P- Δ curves of each filter are linear from applied load of 67 N (15 lb.) to 111 N (25 lb.), so the deflection from 67 N to 111 N was used to calculate the stiffness of the filter. The stiffness (**K**) of seven filters was calculated using the bending test results. The results show that the new Refractron filter has the highest stiffness and the used A-29 Schumacher filter has the lowest stiffness. The filter specimen number from the highest stiffness to the lowest stiffness, in the descending order is: the new 442T Refractron, the new F40 Schumacher, B-27, B-16, B-5, A-23 and A-29. It is noted that the B group specimens are 460 hours used Schumacher filters, and the A group specimens are 1705 hours used Schumacher filters. This shows that bending teat results can reflect the change of the stiffness among

these filters, and this change of stiffness matches with the observation from the vibration tests. However, the measured magnitude of the stiffness from the slope of P-Δ curve is lower than the results from the vibration tests. This is partly due to the resolution of the LVDT measurement and the settlement of the hinge supports in the current bending experiments.

In table 2, it shows the comparison of the frequencies of the A-4 Schumacher filter. The result shows an increase of frequency after being repaired.

Table 2 Comparison of Frequency Before Broken and After Repaired of A-4 Schumacher Filter

	Vibration Mode							
	1	**2**	**3**	**4**	**5**	**6**	**7**	**8**
Before (Hz)	105	287	556	911	1315	1802	2335	2905
After (Hz)	105	293	563	928	1350	1853	2399	3001

Figure 8 shows the first and third mode shape of before broken and after repaired the A-4 damaged filter. In this figure, the X-axis labeled in the position starting from the open end, and the Y-axis represents the normalized FRF. The damaged position is between position 5 (L/2) and position 6 (0.55L).

Application

Results from this study indicate that the vibration signatures of the filters can be used as an index to quantify the mechanical properties of the ceramic candle filters. The application of this study can be implemented to develop a nondestructive evaluation method for future in-situ inspection of the ceramic filters.

Acknowledgements

The authors acknowledge the support provided by the Federal Energy Technology Center, the Department of Energy, for this study under the contracts DE-FG21-97MC34160 and DE-AP21-96MC29319. Special thanks are extended to Mr. Ted McMahon, Dr. T. K. Chiang, Dr. Paul Yue and Mr. Richard Dennis of FETC/DOE for their valuable comments and encouragement. The authors also acknowledge Mr.

Howard Hendrix of Southern Company Services for his help in providing the Coors filter specimens.

References

Alvin, M.A., Tressler, R. E., Lippert, T. E., Diaz, E. S. and Smeltzer, E. E., "Durability of Ceramic Filters," Peper Presented at Coal-Fired Power System 94 – Advances in IGCC and PFBC Review Meeting, 545-571. DOE/METC-94/1008. NTIS/DE94012253. Morgantown, WV, June 1994

Chen, H. L. and Parthasarathy, B., "Evaluating Structural Deterioration of Ceramic Candle Filters Using Dynamic Response", Proceedings of Pittsburgh Coal Conference, September 1996.

Chen, H. L., Spyrakos, C. C., Venkatesh, G., "Evaluating Structural Deterioration by Dynamic Response," Journal of Structural Engineering, Vol. 121, No.8, pp.1197-1204, August 1995.

Spain, J. D. and Starrett, S. H., "Physical, Mechanical, and Thermal Properties of Coors Alumina Mullite Filter Material" Southern Research Institute, August 1994.

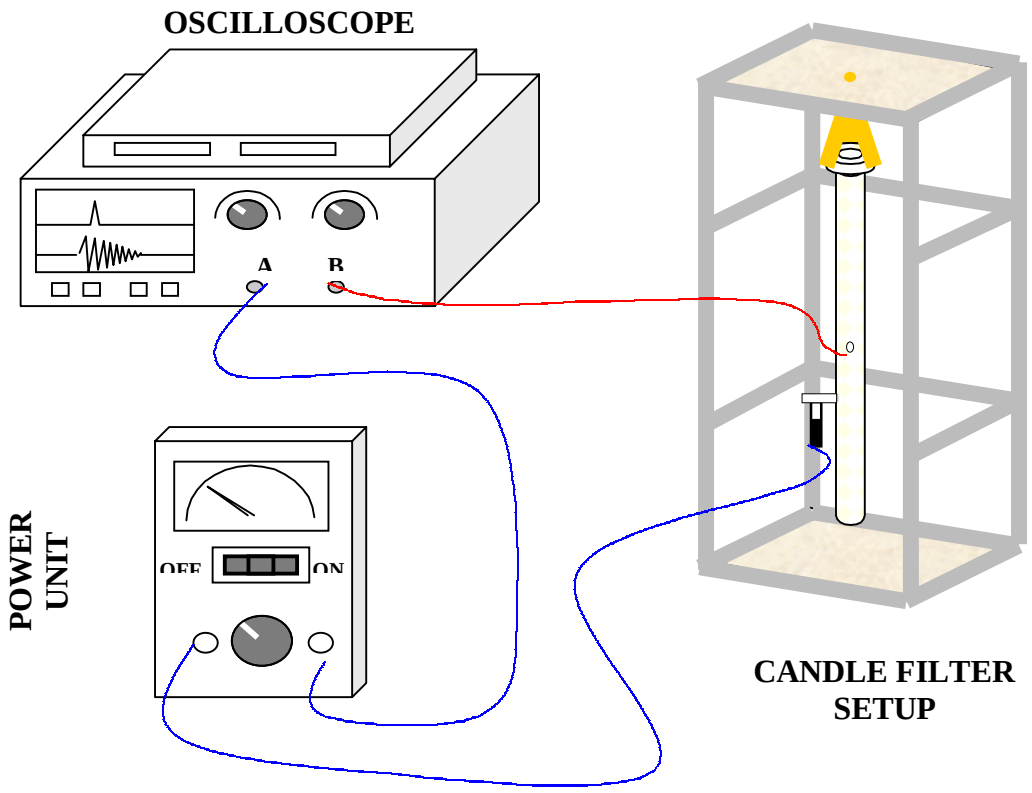

Figure 1 Schematic Drawing of Experimental Setup

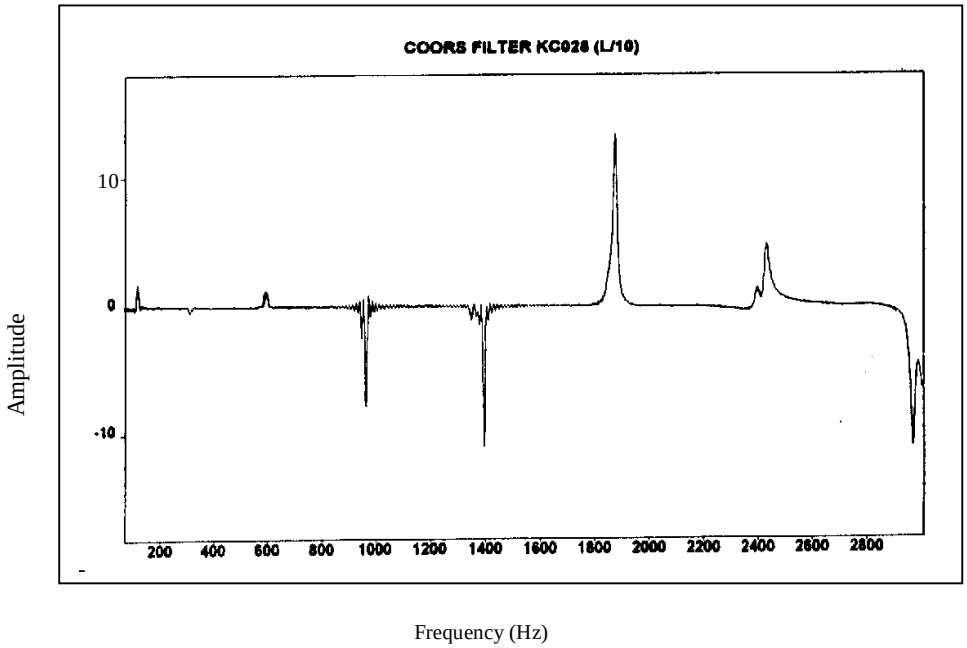

Figure 2. A Typical Frequency Response Function for a Coors Ceramic Filter (Hit point L/10)

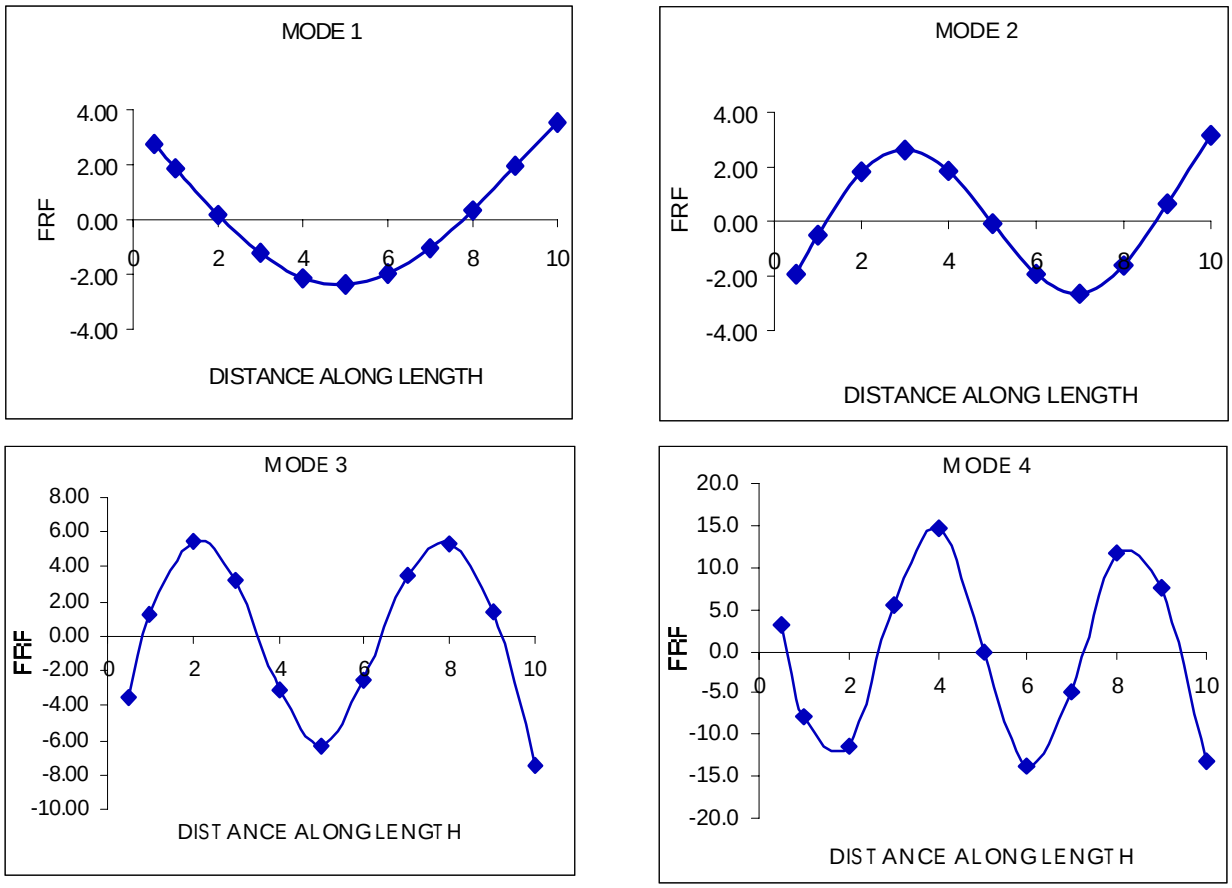

Figure 3 Typical First four Modes Shapes for the Coors Filter (Specimen KC028)

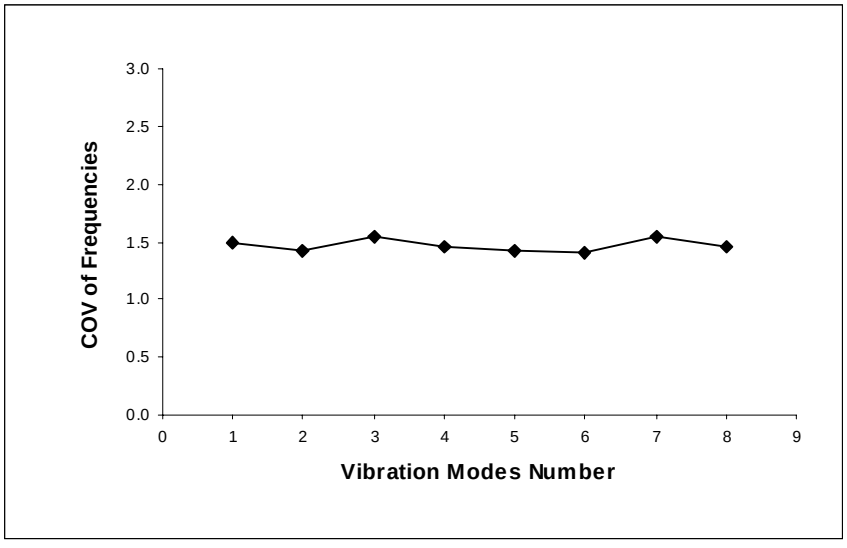

Figure 4 Comparison of COV's for Coors Filters

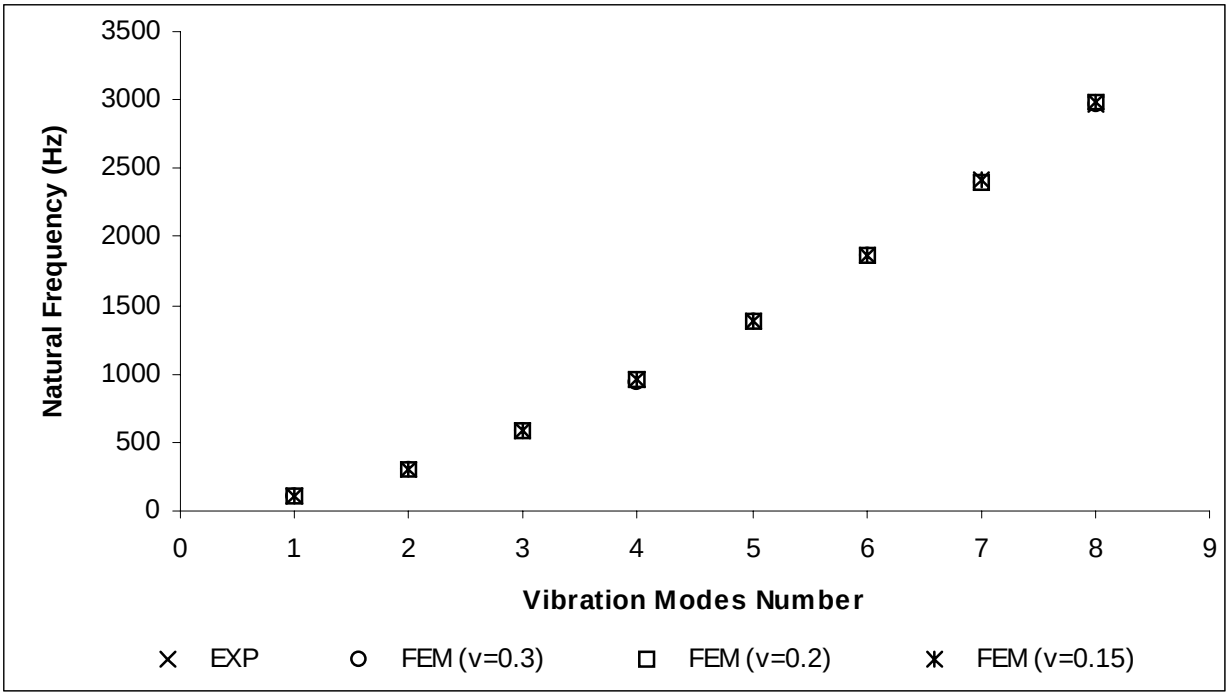

Figure 5 Comparison of Frequencies of experimental and FEM results for Coors Filters

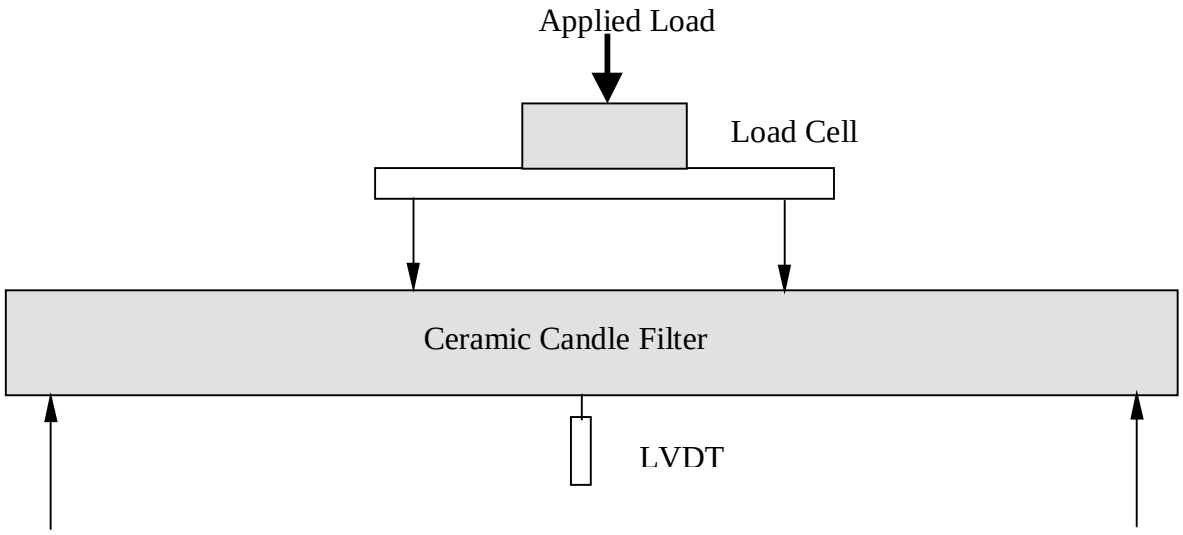

Figure 6 Four Point Bending Test Set-up

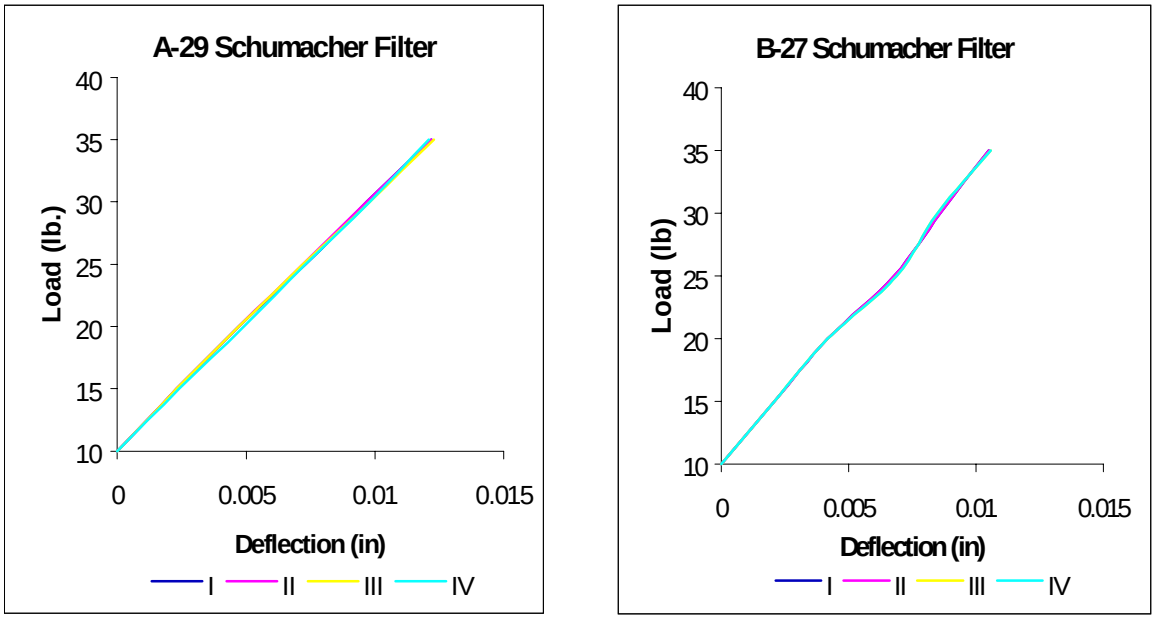

Figure 7 Relationship between Load and Deflection

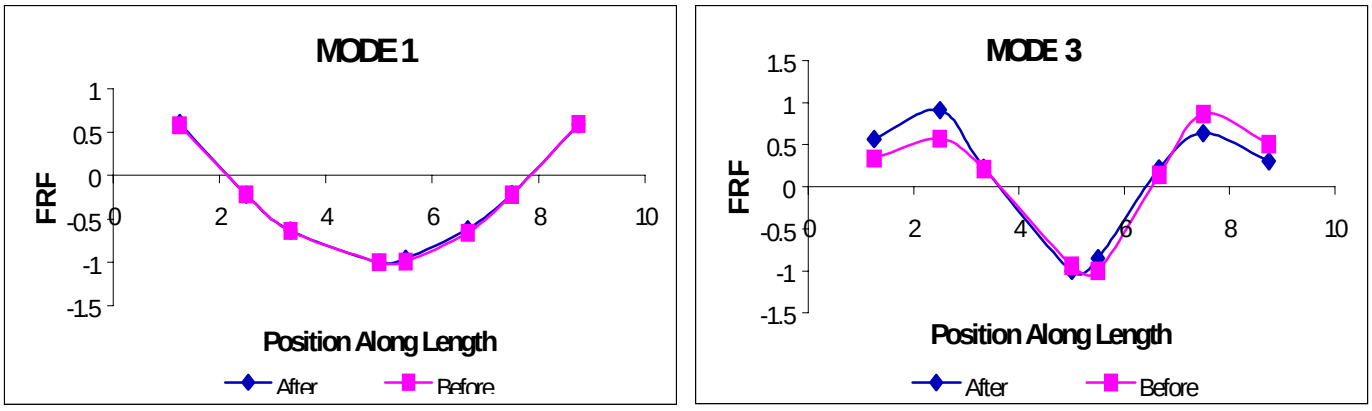

Figure 8 First and third Vibration Mode Shape of the Used Schumacher A-4 Filter